ELSEVIER

Journal of Alloys and Compounds 293–295 (1999) 490–494

Journal of ALLOYS AND COMPOUNDS

Hydrogen-induced stress in Nb single layers

U. Laudahn[a,*], A. Pundt[a], M. Bicker[b], U. v. Hülsen[b], U. Geyer[b], T. Wagner[c], R. Kirchheim[a]

[a]*Institut für Materialphysik, Hospitalstrasse 5, D-37073 Göttingen, Germany*
[b]*I. Physikalisches Institut, Bunsenstrasse 9, D-37073 Göttingen, Germany*
[c]*Max-Planck-Institut für Metallforschung, Seestrasse 92, D-70124 Stuttgart, Germany*

Abstract

Niobium films prepared by molecular beam epitaxy (MBE) and electron beam evaporation (EB) were loaded electrolytically with hydrogen. Out-of-plane strain and in-plane stresses during hydrogen loading were determined using X-ray diffraction and substrate bending measurements. Stress and strain development during loading can be explained using a one-dimensional elastic expansion model up to concentrations of $X_H = 0.05$ H/Nb. Deviations from elastic behavior were observed above $X_H = 0.05$ H/Nb and at $X_H = 0.20$ H/Nb for MBE and EB samples, respectively. These concentrations are where phase separation occurs. Additionally, the stress increase in the EB films deviates from a linear elastic dependence above $X_H = 0.07$ H/Nb within the α-phase. The maximum measured stress is about −2.6 GPa.

Keywords: Hydrogen; Thin film; Stress; Strain

1. Introduction

Hydrogen in thin films has been the subject of recent research [1,2]. The lattice expansion of thin niobium films due to hydrogen absorption is one topic that has been studied by several groups [3–6]. The measured out-of-plane expansion was higher than in the bulk material. This was attributed to the constraints that occur as soon as the film adheres to the substrate. The measurements of Yang et al. [6] on Nb/Pd multilayers showed that the out-of-plane expansion of the clamped films can be well described using linear elastic theory.

The linear elastic model also predicts high in-plane stresses. Thus we present the results of X-ray diffraction measurements to determine the strain, and substrate bending measurements to determine the stress in thin Nb films and compare these results with linear elastic treatment.

2. Experimental details

Our measurements were performed on 190 nm thick Nb films that were prepared by electron beam evaporation at room temperature on Si substrates (EB) and at 900°C on sapphire (MBE).

The EB samples were grown on single-crystal Si substrates at room temperature in a vacuum chamber with a residual pressure of about 10^{-9} mbar. X-ray and texture measurements showed that the films have a strong [110] texture in the growth direction and a random distribution of grain orientations in lateral directions.

The MBE films were grown epitaxially (110)-oriented on Al_2O_3 (1120) substrates. Nb was electron beam evaporated at a substrate temperature of 900°C. The residual pressure was 5×10^{-11} mbar. Texture measurements verified the high quality orientation relation between [111] Nb and [0001] Al_2O_3. Compared with EB films the grain size of the MBE films was much larger.

Both types of Nb film were covered by a 20–30 nm thick Pd top layer at room temperature to prevent oxidation and to facilitate electrochemical charging with hydrogen [6,7]. The hydrogen concentration can be calculated from the measured electric charge using Faraday's law.

The film thicknesses were determined using X-ray reflectometry.

X-ray diffraction measurements were taken in $\Theta/2\Theta$ geometry with a Philips PW-1050 diffractometer using Cu Kα radiation. The out-of-plane lattice parameter was measured at constant hydrogen concentration X_H [H/Nb] between two successive loading steps.

*Corresponding author.

0925-8388/99/$ – see front matter
PII: S0925-8388(99)00471-5

An optical two-beam-deflection setup [8] was used to determine in situ stresses by measuring the bending of the substrate during electrochemical hydrogen charging. The in-plane stress can be calculated using Stoney's equation [9]:

$$\langle\sigma\rangle = \frac{1}{6}\left(\frac{E_s}{1-v_s}\right)\frac{t_s^2}{t_f}\left(\frac{1}{R_0}-\frac{1}{R}\right) \quad (1)$$

where $E_s/(1-v_s)$ and t_s are the biaxial modulus and the thickness of the substrate, respectively, and t_f is the thickness of the film. R_0 and R are the radii of curvature of the substrate before and after hydrogen charging. The resolution of this setup with respect to substrate curvature is better than $\Delta(1/R) = 10^{-4}$ m^{-1} [8].

3. Theory

The expansion of a hydrogen-absorbing film that is clamped on a substrate can be described using linear elastic theory [6,10]. The total out-of-plane strain contains the bulk strain ε_0 and an additional expansion that is generated by the imposed transverse contraction. If elastic anisotropy is considered, this yields [6]:

$$(\varepsilon_{zz})_{total} = \varepsilon_0 + \frac{C_{11}+3C_{12}-2C_{44}}{C_{11}+C_{12}+2C_{44}}\varepsilon_0 \quad (2)$$

where C_{ij} are the elastic stiffness constants of the bulk material. The bulk Nb strain ε_0 shows a linear dependence on the concentration X_H, $\varepsilon_0 = 0.058X_H$ [11]. Using the bulk Nb elastic stiffness constants [12] we can calculate the total expansion $(\varepsilon_{zz})_{total} = 0.136X_H$.

For the calculation of the expected lateral stress, anisotropy has to be taken into account. For the EB sample the random distribution in lateral directions can be considered by averaging the stresses of all lateral directions [13]. The averaged stress is $\sigma = -9.6$ GPa·X_H. For the MBE samples the predicted stress has to be calculated taking the geometry of the sample into account. In our case a stress in the [111] direction $\sigma = -9.0$ GPa·X_H is predicted.

4. Results of strain measurements

Fig. 1 summarizes X-ray patterns of EB Nb films obtained at different hydrogen concentrations. The X-ray pattern of the as-prepared sample ($X_H = 0.00$ H/Nb) shows Nb (110) and Pd (111) lattice reflections. The Pd (111) reflection does not change during hydrogen charging until the Nb is saturated. The Nb (110) lattice reflection shifts with increasing hydrogen concentration towards lower angles due to increasing interplanar spacing. Increasing the H content above 0.20 H/Nb gives rise to the occurrence of another phase with larger out-of-plane spacing. This concentration is much higher than that determined in bulk Nb with $X_H = 0.06$ H/Nb. The relative amount of β-phase increases with total H content. Finally, at a concentration of 0.50 H/Nb the low concentration phase disappears and the whole Nb film is in the β-phase.

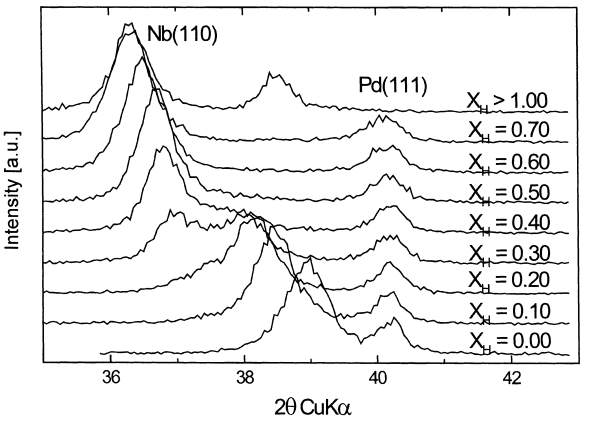

Fig. 1. X-ray patterns of a 190 nm thick EB Nb film with a 30 nm thick Pd top layer during first loading with hydrogen. The marked X_H values give the hydrogen concentration corresponding to each pattern. The Nb (110) peak shifts to lower angles with increasing hydrogen concentration. At 0.20 H/Nb a second Nb–H phase appears, indicating a two-phase region. Above 0.50 H/Nb the α-phase vanishes.

Fig. 2 shows X-ray patterns of the MBE Nb film. The Pd peak remains at the same position with increasing hydrogen concentration. First, the Nb peak shift is comparable to the shift shown in Fig. 1. The second phase occurs at lower concentrations (0.05 H/Nb) than in EB samples. This concentration is approximately the same as in bulk Nb. In the MBE sample the end of the two-phase field is reached at higher concentrations (0.70 H/Nb) compared with the EB sample. In contrast to the EB sample in the two-phase region the Nb reflection remains in a constant position.

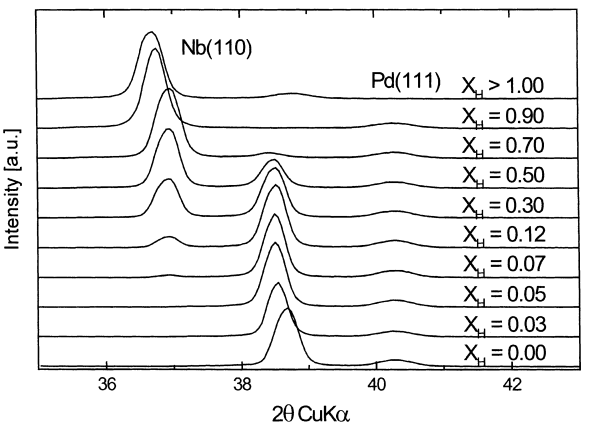

Fig. 2. X-ray pattern of a 189 nm thick MBE Nb film with a 30 nm thick Pd layer. The Nb peak shifts left. Between 0.05 and 0.70 H/Nb a two-phase field exists.

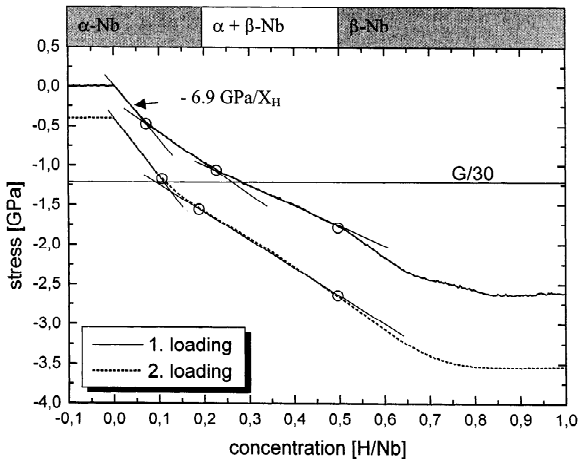

Fig. 3. Stress–concentration curves for the first and second loading with hydrogen of a 190 nm thick EB Nb film. The theoretical shear strength $G/30$ is exceeded. The marked phase boundaries at the top were determined by X-ray measurements. Both stress–concentration curves show three changes in slope. The slope in the elastic range up to 0.07 H/Nb almost follows the calculated stress. The second and third points on each curve can be assigned to the phase boundaries.

5. Results of stress measurements

In-situ stress measurements on an EB Nb film during the first and second loading cycle are presented in Fig. 3. The phase boundaries indicated in the upper part of the figure were determined from X-ray measurements. The starting stress values of both cycles are set arbitrary for a better comparison. The maximum measured overall stress change of -2.7 GPa is higher than the theoretical shear strength $G/30$ of bulk niobium, where G is the shear modulus.[1]

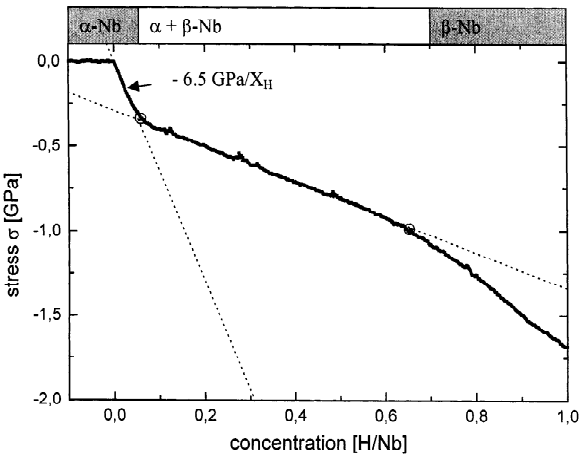

Fig. 4. Stress–concentration curve of a 189 nm thick MBE Nb film. The overall change in stress (-1.6 GPa) is smaller than in measurements of the EB sample. The slope in the α-phase range almost follows the calculated stress. The changes of the slope can be assigned to the phase boundaries, which were determined by X-ray measurements.

[1]It should be mentioned that the theoretical shear strength was obtained from a shear experiment. In our case, compressive stress was applied.

The curves of both loading cycles in Fig. 3 show at least three slope changes marked with circles. The first point of the slope change lies, in both cases, inside the α-phase region. The second point occurs at the beginning, and the third at the end, of the two-phase field. The distance between the first two points narrows during the second loading cycle.

The stress–concentration curve of the MBE Nb film, plotted in Fig. 4, shows only two points of slope change, indicated by circles. These can be assigned to the phase boundaries of the two-phase field, marked at the top of Fig. 4. The maximum measured overall stress change (-1.6 GPa) is lower than for the EB sample.

6. Discussion

From the X-ray patterns (Figs. 1 and 2) we calculated the lattice expansion of the α-Nb (110) plane. A plot of the relative lattice expansion as a function of the hydrogen concentration for the EB Nb film is shown in Fig. 5. Additionally, the lattice expansion of the bulk material (dotted line) and the predicted one-dimensional expansion of a clamped film (dashed line) are shown. In the concentration range up to 0.07 H/Nb, expansion of the film follows the predicted one-dimensional expansion. Thus the film shows linear elastic behavior. Above the critical concentration of 0.07 H/Nb the slope of the curve is lower than predicted. Loading–unloading studies of Pd/Nb multilayers [13] have shown that the Nb diffraction peak is irreversibly shifted in the unloaded state as soon as the critical concentration is passed. Thus, we conclude that the critical concentration $X_H = 0.07$ H/Nb is attributed to the onset of plastic deformation.

Comparable behavior can be seen from the stress measurements, as shown in Fig. 3. In the concentration range up to 0.07 H/Nb the stress almost follows the expected slope as calculated using linear elastic theory.

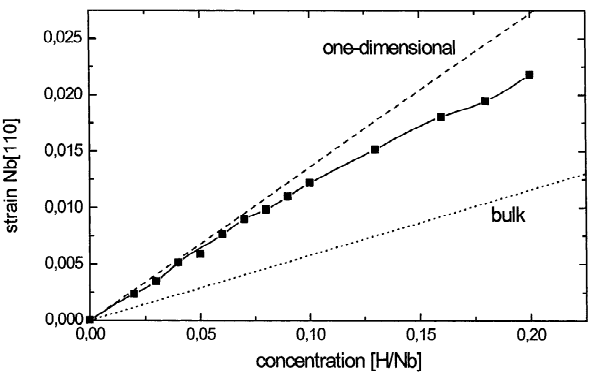

Fig. 5. Relative lattice strain of electron beam evaporated α-Nb as a function of hydrogen concentration. The dashed line was calculated using the one-dimensional elastic model. The dotted line shows the bulk behavior. Up to a concentration of 0.07 H/Nb the measured values follow the model.

The slight deviation in slope might be due to the thin Pd top layer which was neglected in the model. Above X_H = 0.07 H/Nb the slope of the curve is lower, marking the onset of plastic deformation. At the phase boundary concentration of 0.20 H/Nb, taken from the X-ray pattern, the slope of the stress curve is further reduced, indicating the onset of further plastic deformation.

The MBE sample shows different behavior. In Fig. 6 the relative expansion of the α-Nb (110) interplanar distance is plotted as a function of the hydrogen concentration. The strain almost follows the predicted one-dimensional expansion. At the concentration $X_H = 0.05$ H/Nb the second phase appears. The stress measurement, presented in Fig. 6, also shows almost the predicted slope up to 0.05 H/Nb. Above 0.05 H/Nb, the slope of the stress curve decreases and at 0.70 H/Nb it increases again.

Summarizing, the MBE sample behaves linearly elastic in the α-phase and deforms plastically after passing the phase boundary. No plastic deformation takes place within the α-phase.

At the phase boundary a plastic deformation process is activated. Measurements on bulk Nb have shown that, during the formation of misfitting precipitates, extrinsic dislocation loops are emitted [14]. In the case of thin films, such an emission of extrinsic dislocation loops can lead to stress relaxation as soon as the extrinsic dislocation loops are emitted in the out-of-plane direction so that atoms can be transported to the surfaces of the films and the total strain energy can be reduced. After removing the hydrogen this process leaves many dislocations in the sample.

The plastic deformation within the α-phase field, which only occurs in the EB sample, has to be explained by another stress relaxing process. One possible mechanism is the formation of misfit dislocations near the interface between the film and the substrate which also leads to material transport to the film surface. This mechanism is known from the growth of semiconductor films [15,16], but it should also appear in metals. The formation of misfit dislocations in semiconductor films shows a dependence on the misfit between the substrate and the film. In the case of hydrogen-loaded metal films this misfit increases with hydrogen concentration. Thus, the formation of misfit dislocations occurs at a critical H concentration. The formation of the misfit dislocations, and thus the reduction of the stress, depends on the mobility of existing dislocations.

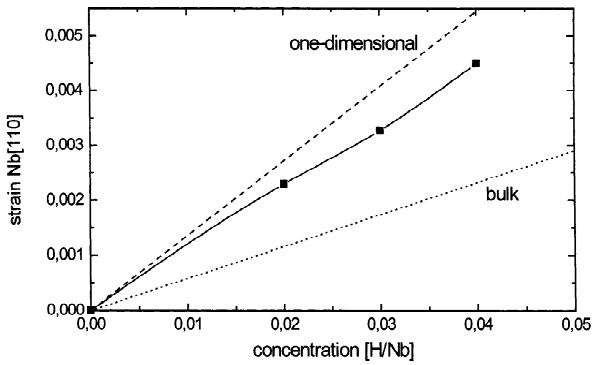

Fig. 6. Relative lattice expansion of a 189 nm thick MBE Nb film. In between the α-phase the strain almost follows the one-dimensional model.

Comparing the first and second loading cycle of the EB sample (see Fig. 3) shows in the latter a shift of the first onset point of plastic deformation to higher concentrations. This can be explained by taking into account the presence of dislocations which were produced during the first loading cycle. These dislocations hinder further formation of misfit dislocations, so that during the second loading cycle a higher hydrogen concentration is necessary to start stress relaxation. This dependence on the dislocation density is predicted in the models [16]. The also predicted dependence on the film thickness will be discussed in another paper [17]. The onset for the second point is correlated with the phase boundary.

The differences between the stress curves of the EB and MBE samples (see Figs. 3 and 4) can also be explained with the relaxation process by taking into account the pile-up of moving misfit dislocations near grain boundaries. The grain size in the MBE sample is larger, so that dislocation pile-up is negligible and stress reduction is maximized. We propose that, because of the good stress relaxation, the shift of the phase boundaries to higher concentrations does not take place in MBE films.

The EB samples have smaller grain sizes and the dislocations can pile up at grain boundaries. The relaxation of the stress is small because of the hindered formation of misfit dislocations. In addition, the maximum measured overall stress change in the EB sample (−2.7 GPa) is higher than in the MBE sample (−1.6 GPa).

7. Conclusion

Strain and stress measurements during the hydrogen charging of Nb films have shown that thin metal films behave linear elastically in a small concentration range. The deviations from elastic behavior at higher concentrations can be explained by plastic deformation processes which are attributed to the occurrence of misfit dislocations near the interface and to the emission of extrinsic dislocation loops during phase transformation. The differences occurring between differently prepared samples (MBE and EB) and between the first and second loading cycle of the EB sample can be explained by these plastic deformation processes.

Acknowledgements

The authors are grateful for the financial support provided by the Deutsche Forschungsgemeinschaft.

References

[1] R. Griessen, J.N. Huiberts, M. Kremers, A.T.M. van Gogh, N.J. Koeman, J.P. Dekker, P.H.L. Notten, J. Alloys Comp. 253 (1997) 44.
[2] Ch. Rhem, F. Klose, D. Nagengast, H. Maletta, A. Weidinger, Physica B 234 (1997) 483.
[3] A. Abromeit, R. Siebrecht, G. Song, H. Zabel, F. Klose, D. Nagengast, A. Weidinger, J. Alloys Comp. 253 (1997) 58.
[4] F. Stillesjö, B. Hjörvarsson, H. Zabel, Phys. Rev. B 54 (1996) 3079.
[5] G. Reisfeld, N.M. Jisrawi, M.W. Ruckmann, M. Strongin, Phys. Rev. B 53 (1996) 4974.
[6] Q.M. Yang, G. Schmitz, S. Fähler, H.U. Krebs, R. Kirchheim, Phys. Rev. B 54 (1996) 9131.
[7] R. Kirchheim, F. Sommer, G. Schluckebier, Acta Metall. 30 (1982) 1059.
[8] M. Bicker, U. von Hülsen, U. Laudahn, A. Pundt, U. Geyer, Rev. Sci. Instr. 69 (1998) 460.
[9] G.G. Stoney, Proc. R. Soc. London, Ser. A 82 (1909) 172.
[10] P.M. Reimer, H. Zabel, C.P. Flynn, A. Matheny, K. Ritley, J. Steiger, S. Blässer, A. Weidinger, Z. Phys. Chem. 181 (1993) 367.
[11] H. Peisl, in: G. Alefeld, J. Völkl (Eds.), Hydrogen in Metals I, Topics in Applied Physics, Vol. 28, Springer, Berlin, 1978, p. 53.
[12] D.I. Bolef, J. Appl. Phys. 32 (1961) 100.
[13] U. Laudahn, Dr. thesis, Cuvillier Verlag Göttingen, 1998.
[14] T. Schober, H. Wenzl, in: G. Alefeld, J. Völkl (Eds.), Hydrogen in Metals II, Topics in Applied Physics, Vol. 29, Springer, Berlin, 1978, p. 32.
[15] J.W. Matthews, A.E. Blakeslee, J. Cryst. Growth 27 (1974) 118.
[16] W.D. Nix, Met. Trans. A 20 (1989) 2217.
[17] U. Laudahn, in preparation.